

A Chemical And Physical Characterization of Alumina-Supported $\text{Rh}_6(\text{CO})_{16}$

KENNETH L. WATTERS, RUSSELL F. HOWE, THOMAS P. CHOJNACKI, CHIA-MIN FU,
ROGER L. SCHNEIDER, AND NING-BEW WONG¹

*Department of Chemistry and Laboratory for Surface Studies, University of Wisconsin-Milwaukee,
Milwaukee, Wisconsin 53201*

Received February 4, 1980; revised May 27, 1980

The decarbonylation and carbonylation reactions of the metal cluster carbonyl $\text{Rh}_6(\text{CO})_{16}$ supported on Al_2O_3 were investigated using volumetric gas adsorption measurements, ir spectroscopy, isotopic measurements, transmission electron microscopy, and EPR spectroscopy. Complete decarbonylation by O_2 and subsequent recarbonylation to $\text{Rh}_6(\text{CO})_{16}$ could be achieved at room temperature provided sufficient physically adsorbed H_2O was present. A two-step reaction scheme is presented which accounts for the experimental data; it is suggested that the Rh_6 cluster remained intact during these reactions. When heated, *in vacuo*, above 250°C , the catalyst lost its ability to undergo the reversible carbonylation/decarbonylation cycle, and the resulting material resembled a highly dispersed conventional Rh catalyst. TEM data showed that no larger crystallites ($>10 \text{ \AA}$) of Rh are formed even when heated *in vacuo* to 450°C .

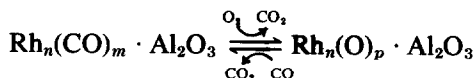
INTRODUCTION

Metal cluster carbonyl compounds continue to be studied as interesting models of surface catalysis and as novel catalyst systems in their own right. A number of reactions have been observed recently which employ metal cluster carbonyls as homogeneous (1) or as heterogeneous (2-6) catalysts.

Both mononuclear and polynuclear metal carbonyls have been observed to undergo rather novel reactions when deposited on various oxide support surfaces (7-17). In general, the complexes appear to lose CO quite readily at room temperature or at slightly elevated temperatures. In some cases this decarbonylation seems to be irreversible, while in other instances the initial compound appears to be reformed by addition of CO. These surface-supported metal species, derived from metal cluster carbonyls, represent a new method of depositing metals on oxide support materials; therefore, it is of interest to study the

nature of the reactions of these metal cluster compounds with the support surface and to determine whether the physical and chemical properties of such supported metal systems are substantially different from the systems formed in the "traditional" manner by depositing metal salts on supports and reducing them at elevated temperatures.

As described in our first paper on this subject (7), a facile reversible decarbonylation occurred when rhodium carbonyl, $\text{Rh}_6(\text{CO})_{16}$, was deposited on alumina. Exposure of the material to oxygen led to a decarbonylated (oxygenated) form which was yellow or tan in color and showed no $\nu(\text{CO})$ bands in the ir spectrum. Placing less than an atmosphere of CO in contact with this oxygenated form slowly regenerated a carbonylated form with a pale violet color and a final ir spectrum much like that of $\text{Rh}_6(\text{CO})_{16}$. Both carbonylation and decarbonylation of the $\text{Rh}/\text{Al}_2\text{O}_3$ material resulted in the formation of CO_2 as shown in the scheme below.



¹ Present address: Department of Chemistry, University of California-Irvine, Irvine, California.

In addition, $\text{Rh}_6(\text{CO})_{16}$ was removed from the alumina into refluxing chloroform (the solvent used for deposition of the complex onto alumina) under a CO atmosphere. We interpreted these observations as evidence for the retention, in some form, of an Rh_6 cluster on the alumina surface during the carbonylation/decarbonylation cycle.

In a recent publication, Smith *et al.* (11) have described an infrared study of $\text{Rh}_6(\text{CO})_{16}$ on ϵ -alumina. They reported the ir spectra obtained for the cluster compound deposited, *in vacuo*, on alumina which had been heated to 200 and 500°C prior to treatment with the chloroform or THF solutions, the observation of the release of H_2 and CO_2 upon contact of Al_2O_3 with $\text{Rh}_6(\text{CO})_{16}$, and spectra obtained when the supported cluster material was heated to 140°C under H_2 and 200°C under CO. Their results indicated that the behavior of the cluster compound on alumina was affected by pretreatment of the alumina and by the presence of air during impregnation. The species they observed exhibited the same general ir features as were reported in our earlier note on the subject (7). These features included bands at ≈ 2050 and 1810 cm^{-1} for the fully carbonylated material, which appeared to be $\text{Rh}_6(\text{CO})_{16}$, and terminal CO bands at ≈ 2090 and 2020 cm^{-1} for a partially carbonylated species. As in our studies, no carbonyl bands were observed below 1800 cm^{-1} . Their ir spectra did show that new spectral features were generated by exposure to H_2 at elevated temperatures. On the basis of their results, they have proposed a reaction scheme to explain the various species observed in the ir spectrum.

In an effort to understand more fully both the nature of the species adsorbed from an $\text{Rh}_6(\text{CO})_{16}$ solution onto an alumina surface, and the reactions which occur when that material reacts with CO or O_2 , we have made quantitative measurements of the adsorption of CO and oxygen and the concomitant formation of CO_2 for several $\text{Rh}_6(\text{CO})_{16}/\text{Al}_2\text{O}_3$ samples. The gas adsorp-

tion data provide evidence regarding stoichiometric relationships between CO and O_2 adsorbed, CO_2 formed, and rhodium content of the samples studied. By using a flow-through ir cell to obtain ir spectra of a sample during gas adsorption measurements, we were able to correlate the ir spectra with points on the gas adsorption curves. In addition, we have used $^{18,18}\text{O}_2$ and D_2O in an effort to elucidate the nature of reactions with the surface-supported cluster, and have studied the adsorption of H_2 on the $\text{Rh}/\text{Al}_2\text{O}_3$ material and the effect of thermal treatment upon the catalyst. We have also obtained transmission electron micrographs to determine the tendency to form rhodium particles in these materials. The results of these investigations are reported here.

EXPERIMENTAL

Preparation of $\text{Rh}_6(\text{CO})_{16}$

All the hexarhodium hexadecacarbonyl used in this study was prepared from $[\text{Rh}(\text{CO})_2\text{Cl}]_2$ using the atmospheric pressure synthesis described by Chini and Martinengo (18). The dark brown methanol insoluble product of the preparation was purified by repeated recrystallization from chloroform to give dark violet crystals. Elemental analysis and infrared spectroscopy were used as routine measurements of purity.

Description of Volumetric System

The manometry was conducted on a glass-metal hybrid high vacuum line equipped with a recirculation loop. Background pressures of less than 10^{-5} Torr routinely were obtained prior to introduction of reactant gases. Recirculation of the reactant gases was achieved with a metal bellows pump and the flow rates were controlled by a needle valve. Pressure measurements were made using a constant volume manometer-cathetometer combination. All reactant gases, which were purified by standard methods, were

introduced from permanently attached glass storage bulbs into a calibrated volume section of the recirculation loop. The manometric measurement of condensable product gases was accomplished by selective trapping with appropriate cyrostats followed by quantitative transfer to the calibrated volume section.

Preparation of Supported Material on $\gamma\text{-Al}_2\text{O}_3$

The $\gamma\text{-Al}_2\text{O}_3$ -supported hexarhodium hexadecacarbonyl catalysts were prepared by the chloroform solution impregnation method described earlier (7) with the exception that the impregnations were carried out at room temperature from a slurry of alumina in the chloroform solution of $\text{Rh}_6(\text{CO})_{16}$. The alumina, supplied by Akzo Chemie bv (CK-300, 25-80 mesh), had a surface area of $200 \text{ m}^2/\text{g}$, as established by BET measurements. The alumina had been calcined at 500°C to remove organics, but was subsequently exposed to atmosphere.

Concentrations and volumes of the subsaturated chloroform solutions of $\text{Rh}_6(\text{CO})_{16}$ were adjusted to produce yellow to tan supported catalysts with Rh loadings varying from 0.6 to 7% by weight. Adsorption of the rhodium carbonyl out of chloroform onto the alumina was judged to be complete when the chloroform became colorless. The observation of the disappearance of color of the CHCl_3 solution thus provided an estimate of an upper limit of the Rh loadings.

The $\text{Rh}/\text{Al}_2\text{O}_3$ materials were filtered and dried in air for several hours. An analysis of a 1.65 wt% Rh sample prepared in this way showed a chlorine content of 0.35 wt%.

The dried $\text{Rh}/\text{Al}_2\text{O}_3$ powders were pressed into 1-in.-diameter wafers at 30,000 psi. The 150–200 mg wafers were cut into $1 \times 1 \text{ mm}$ chips for use in bulk manometric measurements and into $1 \times 2 \text{ cm}$ rectangles for use in infrared measurements.

ir Spectra

Infrared spectra were obtained using a

Beckman IR-12 spectrophotometer in the double beam mode. Gain and slit adjustments were made to bring the single beam energy level to 50–60% in the 2000 cm^{-1} region before recording the double beam spectrum. Spectral slit widths are $2\text{--}5 \text{ cm}^{-1}$ for all samples. The specially designed cell shown in Fig. 1 was used to measure simultaneously ir spectra and gas adsorption on a single catalyst.

TEM Studies

Micrographs were obtained at Eastman Kodak Research Laboratories in Rochester, New York, by G. Apai and J. Hamilton. The microscope was a Zeis EM10. Under the conditions employed, metal particles of 10 \AA diameter would have been resolved on the alumina samples.

EPR Spectra

EPR spectra were obtained on a Varian E115 spectrometer operating at 99 Hz. Samples were contained in a high vacuum cell fitted with a quartz sidearm, and spectra

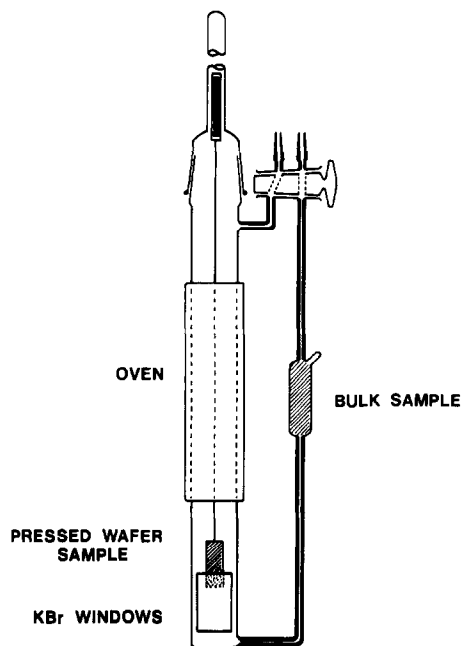


FIG. 1. Sample cell employed for simultaneous gas adsorption and ir spectral measurements.

were recorded at 77 K and room temperature.

Isotopic Studies

$^{18,18}\text{O}_2$ was 99.9% and was purchased from Prochem. Mass spectral analyses were obtained using a Hitachi-Perkin Elmer RMU 6 D or AEI MS10 mass spectrometer. Most isotopic studies were conducted by placing the reactant gases in contact with the sample in a static system for a period of time, then removing an aliquot of the gases for mass spectral analysis. When it was desired to minimize contact of the CO_2 product with the alumina surface, a continuously recirculating system was used and the CO_2 was trapped in a liquid N_2 trap on each cycle.

RESULTS

Gas Adsorption Measurements

Figure 2 shows results obtained for a typical CO adsorption experiment in which CO was added to the decarbonylated form

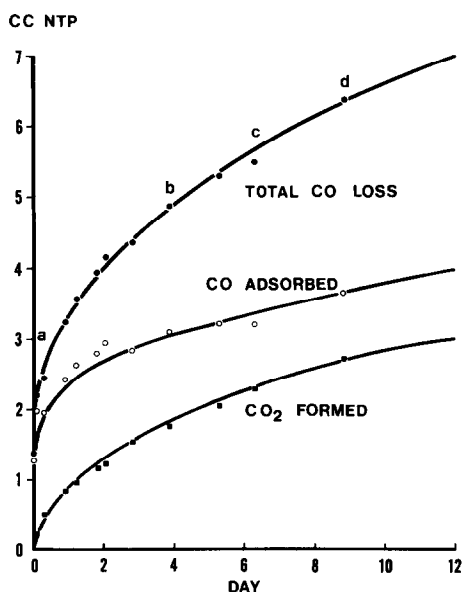


FIG. 2. Plot of gas adsorption data for the carbonylation of a sample containing 2.01 g of 0.7% Rh on Al_2O_3 . Points labeled a, b, c, d represent points for which data in Fig. 7 were obtained.

of the $\text{Rh}/\text{Al}_2\text{O}_3$ material. The rapid initial physical adsorption of CO represented only a small fraction of the total CO adsorption on these samples; all data were corrected for this physisorption. The total volume of gas present was measured for each determination and the contribution of CO_2 to the total was then obtained by trapping CO_2 at 77 K. No evidence was obtained from gas chromatography or mass spectrometry for the presence of gases other than CO and CO_2 during the carbonylation process.

As may be seen in Fig. 2, the chemisorption of CO in the *early stages* of the experiment was accompanied by the formation of only small quantities of CO_2 , while the rate of CO_2 formation relative to CO adsorption increased dramatically in the later stages of the experiment. The solid curve of Fig. 3 shows the ratio of $\text{CO}(\text{ads})/\text{CO}_2(\text{formed})$ as a function of time for the experiment represented in Fig. 2. The convergence of this ratio to 1.3 was typical of the carbonylation cycle for each sample studied if the sample had been treated only at room temperature.

Early experiments had suggested that the degree of hydration had a substantial effect upon the rate of the carbonylation process.

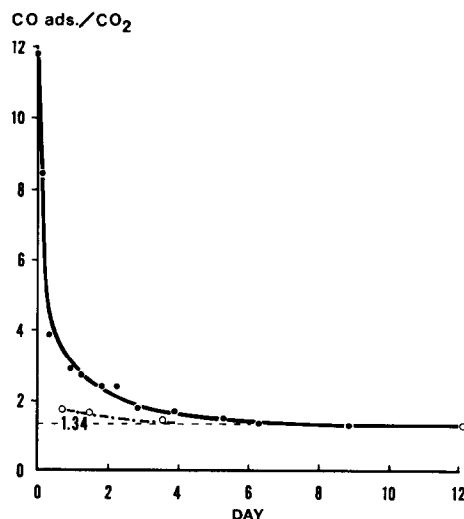


FIG. 3. Plot of the ratio $\text{CO}(\text{ads})/\text{CO}_2(\text{formed})$. Solid curve is for the data in Fig. 2; dashed curve for the data in Fig. 4.

This also has been reported by others (11). To confirm this we added water vapor to a fully oxygenated sample and allowed the vapor to circulate through the sample for several hours. The remaining water vapor was then condensed in a dry ice trap and CO was admitted to the system in a static mode to measure its chemisorption and the formation of CO₂. Figure 4 shows the results obtained in this experiment. The rate of the carbonylation was significantly enhanced and initial rate of production of CO₂ was far greater than for the study shown in Fig. 2 where the sample had far less water content. The dashed curve of Fig. 3 shows the CO(ads)/CO₂(formed) ratio for this sample. As may be seen, the approach to 1.3 occurred much earlier in the carbonylation process for this sample. Table 1 presents the CO(ads) and CO₂

formation data for the several samples on which the measurements were made.

Our infrared experiments had also shown (7) that a carbonylated sample could be completely decarbonylated by exposure to O₂; the presence of sufficient water in the system is important, however, to facilitate this process. Figure 5 presents the gas volume curves as a function of time for a fully carbonylated sample exposed to O₂. Immediate and rapid formation of CO₂ occurs along with adsorption of O₂ by the sample over the first few hours. After about 2 days there was very little change in the measured gas volumes even though the ir spectrum indicated the decarbonylation was not complete (*vide infra*). After 100 hr we had formed about 1.03 mol of CO₂ and adsorbed about 0.82 mol of O₂ per Rh atom in the sample.

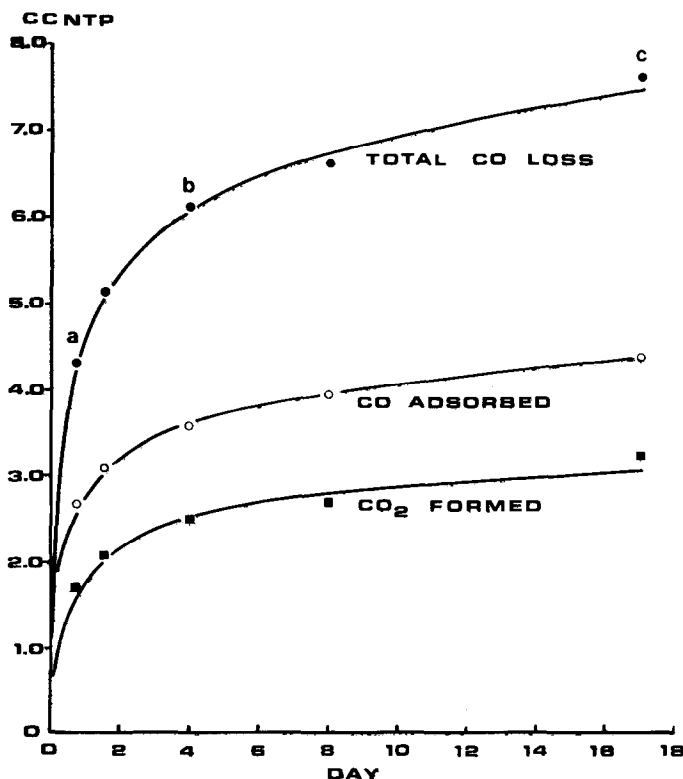


FIG. 4. Plot of gas adsorption data for the carbonylation of a sample saturated with water by the introduction of equilibrium vapor pressure of H₂O. Sample contained 2.01 g of 0.7% Rh on Al₂O₃. Points a, b, c correspond to points at which ir spectra in Fig. 8 were obtained.

TABLE 1
Summary of CO Adsorption Data

Sample	CO(ads)/Rh	CO ₂ (prod.)/Rh	CO(ads)/CO ₂ (prod.)
0.58 g of #1 ^a	1.04	0.775	1.34
0.54 g of #1	1.00	0.763	1.32
1.38 g of #2	1.65	1.27	1.30
1.01 g of #2	1.63	Not determined	Not determined
2.01 g of #3 ^b	0.86	0.64	1.34
1.33 g of #3 ^c	1.52	1.12	1.35

^a All samples prepared by depositing $\text{Rh}_6(\text{CO})_{16}$ on $\gamma\text{-Al}_2\text{O}_3$. Sample #1 = 7.3% Rh; sample #2 = 0.86%; sample #3 = 0.70% Rh.

^b Adsorption measurement initiated prior to complete decarbonylation (oxygenation) of sample.

^c Adsorption measurement made after introduction of water vapor to saturate alumina surface.

Titration of an oxidized or oxygenated sample with hydrogen may be used to obtain information about the mode of interaction of oxygen with the surface and the quantity of oxygen bound to the surface. Figure 6 shows the data obtained for adsorption of H_2 on a sample which had been oxygenated until no $\nu(\text{CO})$ spectrum remained. The hydrogen was taken up in two stages; the reaction was terminated when H_2/Rh was 2.1. The sample was then evacuated to 10^{-6} Torr and reexposed to H_2 . Only the rapid first stage of the H_2 adsorption was observed in this second experiment (curve B) and the final H_2/Rh was 0.9.

Infrared Spectra

In order to understand the nature of the reactions occurring in the rhodium carbonyl/alumina systems it was important to couple the gas adsorption measurements with the ir spectra of the samples at various states of carbonylation. During a carbonylation such as that represented in Fig. 2, we obtained ir spectra every few hours. Figure 7 shows the spectra obtained at various stages along the carbonylation cycle. Each spectrum corresponds to a set of points in the gas adsorption curve of Fig. 2. As may be seen, the pair of peaks at 2090 and 2020 cm^{-1} develop during the very early stages

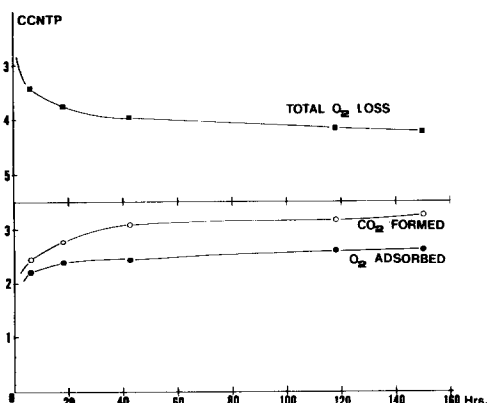


FIG. 5. Plot of gas adsorption curves for oxygenation of a fully carbonylated sample. Sample contained 2.01 g of 0.7% Rh on Al_2O_3 .

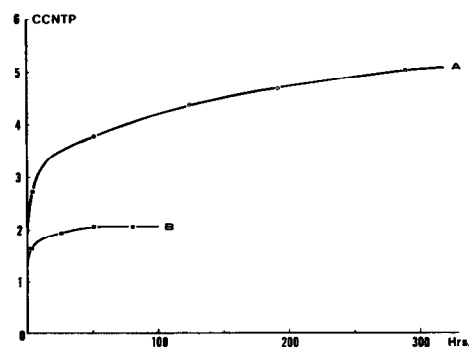


FIG. 6. Plot of adsorption of H_2 on 1.87 g of 0.60% Rh on Al_2O_3 . Curve A is gas adsorbed upon initial exposure of sample to H_2 ; curve B is H_2 adsorbed after evacuation to 10^{-6} Torr followed by reexposure to H_2 .

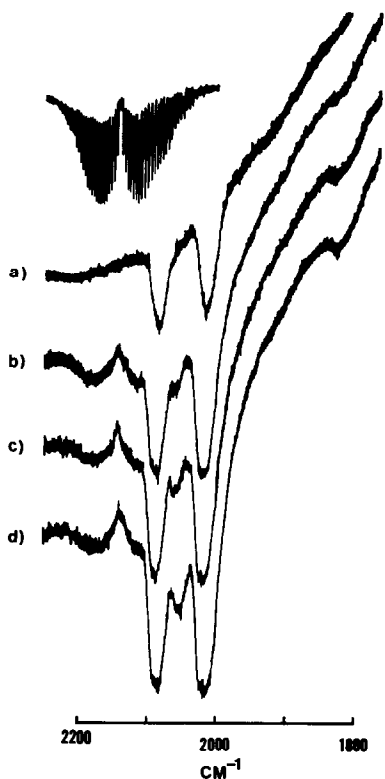


FIG. 7. Ir spectra obtained during carbonylation represented by gas adsorption plots of Fig. 2. Spectra a, b, c, d were taken at times indicated by the corresponding points in Fig. 2. The CO gas phase spectrum is shown above spectrum (a) for comparison with the feature near 2140 cm^{-1} in spectra b-d.

of carbonylation. These peaks grow in intensity and are the only $\nu(\text{CO})$ peaks through about the first 75% of the CO adsorption shown in Fig. 2. Only after about 50 hr are a terminal peak near 2060 and a bridging peak near 1815 observed (Fig. 7c). About one-third of the CO_2 formation has occurred by the time spectrum 7c is first observed; the ratio of $\text{CO}(\text{ads})/\text{CO}_2(\text{formed})$ approaches 1.3 only after appearance of these new peaks. These new terminal and bridging peaks increase in intensity until the end of the period of observation covered in Figs. 2 and 7. This infrared evidence shows at least two stages occurring during carbonylation of the supported rhodium carbonyl sample. In stage I, the two terminal peaks at 2090 and 2020

cm^{-1} are present; CO_2 formation is slow relative to CO adsorption during this stage of the reaction. During stage II, peaks at 2060 and 1815 cm^{-1} develop and most of the CO_2 formation occurs.

We also investigated the effect of water saturation upon the development of various stages of the ir spectrum for these materials. Figure 8 shows ir spectra obtained for a sample during the gas adsorption measurements represented in Fig. 4 where the sample was water saturated. The $\nu(\text{CO})$ peaks typical of stage II of the carbonylation process are observed as the major bands for the sample soon after initiation of the experiment while the bands typical of stage I are present only as shoulders even in the first spectrum obtained.

The reverse reaction, decarbonylation with O_2 , was also followed by ir while gas adsorption measurements were being conducted. As is mentioned above, circulation of dry O_2 through a fully carbonylated sample produced CO_2 and some O_2 was adsorbed but the reaction stopped well before the sample had been completely decarbonylated. Figure 9 shows the spectra of this sample prior to addition of O_2 and after recirculation for the 150 hr represented by Fig. 4, by which time the reaction appeared to have stopped. Water vapor (10 Torr) was then added to the system and the ir spectrum recorded after about 4 more hr exposure to O_2 . Spectrum 9c shows that all carbonyl bands had disappeared from the spectrum by this time. Exposure to water vapor alone caused no decarbonylation.

In order to study the thermal stability of the alumina-supported rhodium carbonyl materials, a sample was treated at elevated temperatures, then exposed to CO or CO and H_2O . When a fully carbonylated sample was outgassed while heating at 150°C it was converted to a sample with the terminal CO bands at 2090 and 2020 cm^{-1} (Fig. 10) which are typical of the stage I species of the carbonylation process. Addition of CO alone was not sufficient to regenerate the fully carbonylated material, but CO and

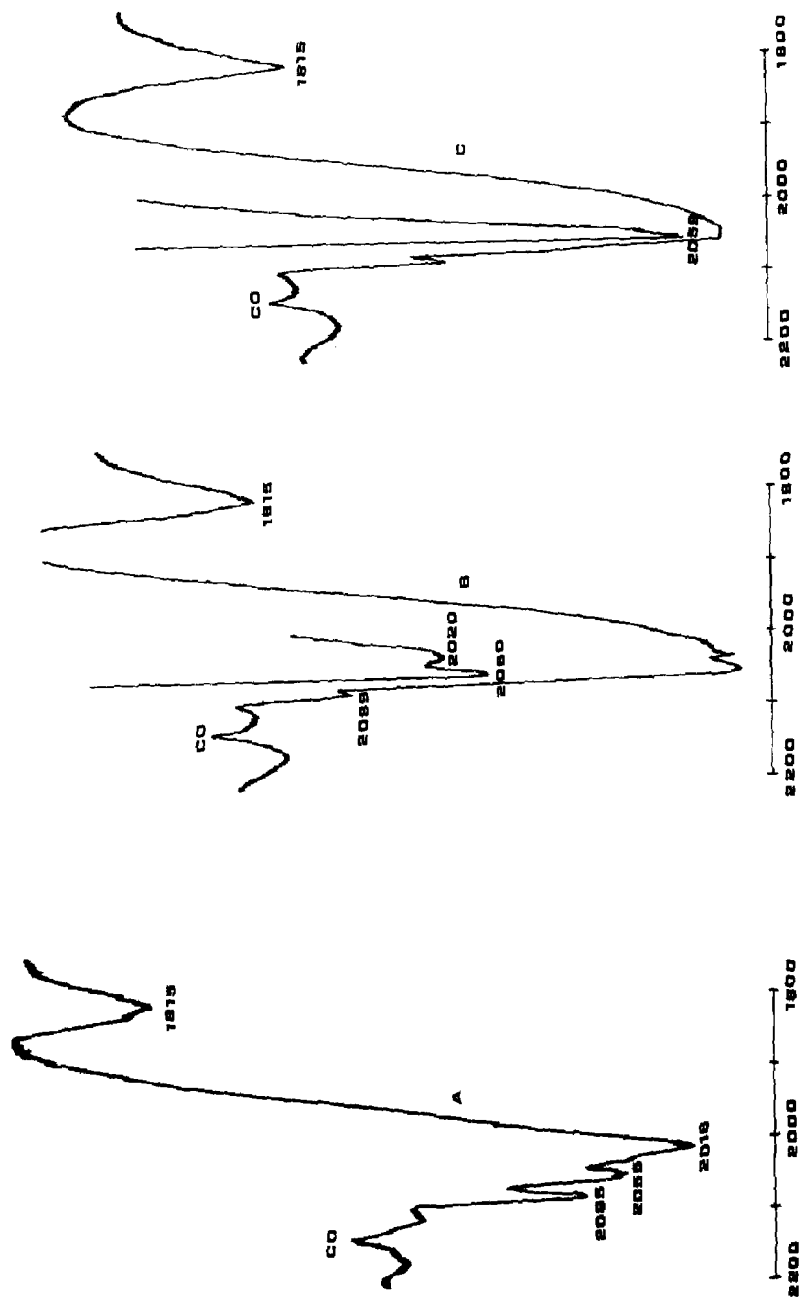


Fig. 8. Ir spectra obtained during carbonylation of wet sample as represented by gas adsorption plots of Fig. 4. Spectra a, b, and c were taken at times indicated by corresponding points in Fig. 4.



FIG. 9. Ir spectra obtained during oxygenation of a carbonylated sample as represented by gas adsorption plots of Fig. 5. Spectrum (a) is spectrum prior to introduction of O_2 ; spectrum (b) is after 150 hr exposure to O_2 (see Fig. 5); spectrum (c) is for the sample in (b) but after introduction of H_2O at equilibrium vapor pressure.

H_2O produced a species with ir spectrum typical of the fully carbonylated form in just 2 hr.

By contrast, a sample heated to $250^\circ C$ while outgassing was completely decarbonylated. Exposure to CO followed by CO and H_2O for an extended period produced only the two terminal CO bands typical of the intermediate species except that they were observed at higher frequencies (2105 and 2030 cm^{-1}) than those for the unheated sample. No trace of the terminal and bridging bands typical of the fully carbonylated sample was observed. The same behavior was observed for a sample outgassed at $400^\circ C$. The $\nu(CO)$ frequencies obtained in these studies are summarized in Table 2.

Electron Micrographs

Examination of $\gamma\text{-Al}_2\text{O}_3$ -supported rhodium carbonyl samples of about 1 wt% Rh disclosed no evidence of rhodium particles larger than 10 \AA diameter in any of the micrographs. The samples studied included both those treated only at room temperature and those heated *in vacuo* at temperatures up to $450^\circ C$.

Isotopic Studies

To obtain more information regarding the nature of the reactions occurring between gas phase species and the Rh/ Al_2O_3 surfaces, a series of experiments was conducted using $^{18,18}O_2$. Table 3 lists the measured ratios of the important isotopic species in these experiments.

In the first experiment, a fully decarbonylated (oxygenated) Rh/ Al_2O_3 sample was exposed to an equimolar mixture of $^{18,18}O_2$ and $^{16,16}O_2$. The final ratios of masses 32, 34, and 36 indicated that exchange between the gas phase oxygen and ^{16}O on the rhodium surface had occurred, but there had been no scission of O-O bonds to produce $^{16,18}O_2$.

In a second experiment, $^{18,18}O_2$ was added to a sample which had been fully carbonylated with $C^{16}O$. The oxygen remained in static contact with the solid for 2

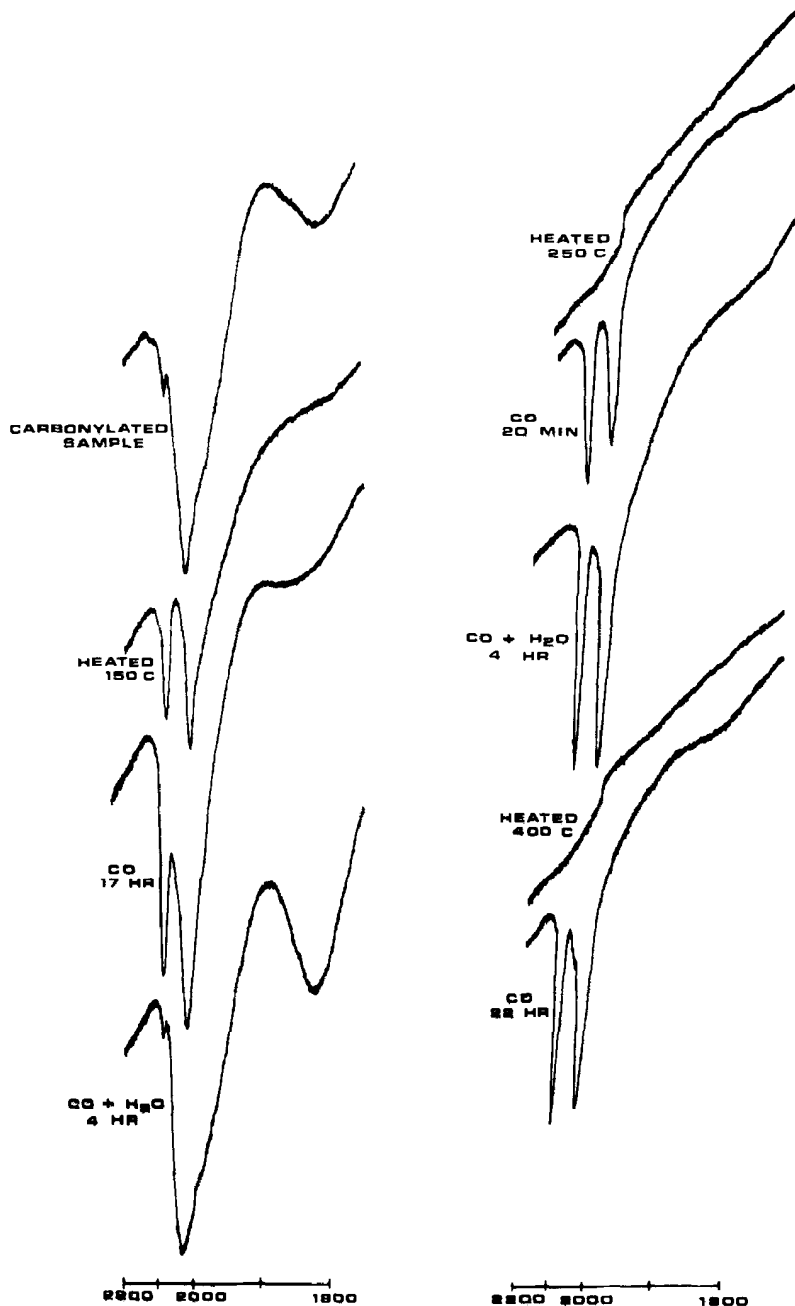


FIG. 10. Ir spectra for sample outgassed at elevated temperatures.

days. The CO_2 formed was predominantly mass 44, but contained significant amounts of mass 46 and 48. The O_2 remaining in the gas phase after the reaction was predominantly mass 36.

Finally, a fully oxygenated sample was

exposed to a stoichiometric mixture of $^{18,18}\text{O}_2$ and C^{16}O . The pressure in the gas phase approached two-thirds the value of the initial gas pressure after 2 days indicating the reaction $2\text{CO} + \text{O}_2 \rightarrow 2\text{CO}_2$ had neared completion. Mass spectral analysis

TABLE 2
 CO Frequencies^a

Description of system	Terminal $\nu(\text{CO})$	Bridging $\nu(\text{CO})$
Fully carbonylated—room temperature (Species C) ^b	2060	1815
Partially carbonylated—room temperature (Species B) ^b	2090, 2015	—
Sample outgassed at 150°C ^c	2090, 2015	—
Sample outgassed at 150°C followed by exposure to H ₂ O + CO ^c	2050	1820
Sample outgassed at 250°C followed by exposure to H ₂ O + CO ^c	2105, 2030	—
Sample outgassed at 400°C followed by exposure to H ₂ O + CO ^c	2105, 2030	—
Fully carbonylated sample which was oxygenated for 150 hr	2087, 2015	—
Rh ₆ (CO) ₁₆ (crystalline)	2060, 2025	1805

^a Frequencies in cm⁻¹.

^b For explanation of species B and C see Discussion section.

^c All samples were outgassed at <10⁻⁵ Torr.

again showed that the CO₂ formed was predominately mass 44 but was enriched in masses 46 and 48. The O₂ remaining was predominantly mass 36.

Similar results were obtained when a sample oxygenated with ³⁶O₂ was reacted with the stoichiometric mixture of ³⁶O₂ and CO (last entries in Table 3). In the two separate experiments of this type, we first dehydrated the sample and recirculated the reactant gases through it, trapping CO₂ on each cycle to minimize contact of CO₂ with water on the alumina surface; in the second experiment we allowed the product CO₂ to remain in static contact with a relatively wet sample. The first experiment produced increased quantities of mass 46 and mass 48 CO₂ as compared with the second experiment.

EPR Spectra

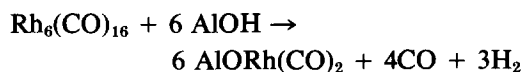
EPR spectra were recorded at 77 K for Rh₆(CO)₁₆/Al₂O₃ (0.86% Rh by weight) in both the fully carbonylated and decarbonylated states. Two very low intensity signals were obtained from the decarbonylated state $g_{\parallel} = 2.10$ and 2.05 , $g_{\perp} \approx 1.99$ which could be enhanced by heating the sample in

O₂. These signals are most probably due to Rh²⁺, or, alternatively, O₂⁻ formed on rhodium sites (19). The total integrated intensities however corresponded to less than 5% of the Rh present, and the spectra were thus not investigated in detail.

DISCUSSION

Initial Decarbonylation of Adsorbed Rh₆(CO)₁₆

Smith *et al.* (11) have suggested that the initial adsorption of Rh₆(CO)₁₆ from solution onto an alumina support involves oxidation of the complex by surface hydroxyl groups:



In our experiments, adsorption of Rh₆(CO)₁₆ was always carried out in an open system exposed to air, so that we cannot distinguish between oxidation by the surface or by molecular oxygen. However, the reaction suggested by Smith *et al.* (11) seems unlikely for two reasons. There is no evidence that the hydroxyl groups on alumina are able to oxidize zerovalent car-

TABLE 3
 Isotopic Reaction Data

Reaction	Ratio	Ratio
	C ^{16,18} O ₂ : C ^{16,18} O ₂ : C ^{18,18} O ₂	^{16,18} O ₂ : ^{18,16} O ₂ : ^{18,18} O ₂
^{16,16} O ₂ + ^{18,18} O ₂ + Rh(¹⁶ O)/Al ₂ O ₃ ^a	—	1.1 : 0.006 : 1.0 ^b
^{18,18} O ₂ + Rh(C ¹⁶ O)/Al ₂ O ₃ ^c → CO ₂	1.0 : 0.08 : 0.02	1.0 : 0.116 : 480
^{18,18} O ₂ + 2C ¹⁶ O + Rh(¹⁶ O)/Al ₂ O ₃ → 2CO ₂	1.0 : 0.16 : 0.008 ^d	1.0 : 0.03 : 60
^{18,18} O ₂ + 2C ¹⁶ O + Rh(¹⁸ O)/Al ₂ O ₃ → 2CO ₂	1.0 : 0.27 : 0.02 ^e	—
	1.0 : 0.1 : 0.01 ^f	

^a Rh(¹⁶O)/Al₂O₃ indicates a sample oxygenated with natural abundance O₂.

^b The initial quantity of O₂(ads) on the Rh/Al₂O₃ corresponded to about 5% of the total O₂ in the gas phase; the initial gas phase ratio ³²O₂/³⁶O₂ = 1.0.

^c Rh(C¹⁶O)/Al₂O₃ indicates a sample fully carbonylated with natural abundance C¹⁶O.

^d Values obtained under static conditions without trapping CO₂.

^e Values obtained for a dehydrated sample with CO₂ continuously trapped.

^f Values obtained after addition of water and without trapping CO₂ continuously.

bonyl complexes at room temperature. For example, Mo(CO)₆ (12), Ni(CO)₄ (20), Fe₂(CO)₉ (13), and Fe₃(CO)₁₂ (13) have all been shown to be oxidized only on heating *in vacuo*. The H₂ observed in (11) during initial adsorption from solution may be due to reaction with adsorbed water, or to reaction of the solvent with the alumina support. Furthermore, the observation (11) that adsorbed Rh₆(CO)₁₆ is more stable on alumina supports dehydrated at 200 or 500°C is not consistent with hydroxyl groups being the oxidizing species. Dehydration at 200°C will not appreciably dehydroxylate the alumina, and even after dehydration at 500°C alumina still contains a sufficient concentration of hydroxyl groups to oxidize adsorbed Mo(CO)₆ when the Mo(CO)₆/Al₂O₃ is heated above 200°C (12).

We prefer to believe that the rapid and complete decarbonylation that occurs when Rh₆(CO)₁₆ is adsorbed from solution onto alumina in air is associated with the presence of O₂ and H₂O. In our experiments, O₂ is readily available during adsorption of Rh₆(CO)₁₆. In the experiments of Smith *et al.* (11) complete decarbonylation during initial adsorption of Rh₆(CO)₁₆ also was observed when air was present, but, on alumina supports which had been outgassed prior to adsorption *in vacuo*, the decarbonylation did not go to completion,

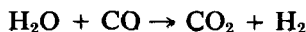
and the stability of adsorbed Rh₆(CO)₁₆ increased with increasing pretreatment temperature of the support. This follows from our observation, to be discussed further below, that removal of physically adsorbed H₂O from a previously prepared sample of Rh₆(CO)₁₆ on Al₂O₃ retards the decarbonylation of the sample to a considerable extent.

Carbonylation and Decarbonylation Cycles

The reaction of CO with the decarbonylated (oxygenated) form of Rh₆(CO)₁₆ on alumina after preparation in air is clearly a two-step process. The infrared spectra obtained here are very similar to those reported by Smith *et al.* (11). The pair of carbonyl bands at 2090 and 2020 cm⁻¹ that appear in the first step were assigned by Smith *et al.* (11) to an oxidized dicarbonyl species Rh⁴(CO)₂. Such an assignment seems reasonable, in view of the close similarity of the spectrum to that of (Rh(CO)₂Cl)₂ (7). It must be pointed out, however, that there are considerable differences of opinion in the literature as to the nature of the rhodium dicarbonyl species that are formed on a variety of rhodium catalysts. For example, J. T. Yates *et al.* (21) have recently assigned a pair of car-

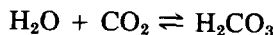
bonyl bands at 2104 and 2034 cm^{-1} on a conventional Rh-Al₂O₃ catalyst to a dicarbonyl species formed at single rhodium atom sites, whereas D. Yates and co-workers (22) have suggested that the dicarbonyl species is formed at the edges of larger metal clusters observed by electron microscopy. Primet has assigned the same bands to an oxidized species, Rh(CO)₂ (23), and similar bands have been observed in rhodium-exchanged zeolites containing Rh^I and Rh^{III} cations (24). Thus, from the carbonyl spectrum alone, it is not possible to unambiguously characterize the dicarbonyl species formed in the first step of the reaction of CO with the oxygenated Rh₆(CO)₁₆-Al₂O₃ catalysts. From our volumetric data, it is clear that not all of the rhodium present in the oxygenated samples is able to react with CO to form a dicarbonyl species. Even for the fully carbonylated samples at low loading the maximum CO(ads)/Rh value obtained in our experiments was 1.7.

The second step in the carbonylation reaction is associated with the formation of CO₂ and the appearance of infrared bands at 2060 and 1815 cm^{-1} characteristic of Rh₆(CO)₁₆. This step is normally very slow, but is considerably accelerated in the presence of physically adsorbed H₂O. The possibility of CO₂ being formed via the water gas shift reaction:



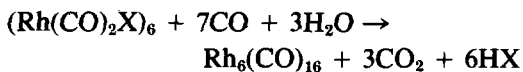
can be dismissed, since no traces of H₂ were detected during the reaction, and the infrared spectra showed no evidence of adsorbed hydrogen (either Rh-H stretching bands, or shifts in carbonyl bands due to formation of hydridocarbonyl species (28, 29)). The remarkably constant ratio of CO adsorbed to CO₂ produced (Table 1) requires that all rhodium adsorbing CO is involved in the reaction leading to CO₂ production, otherwise the ratio would differ from sample to sample. The constant ratio with samples containing different loadings

of rhodium also indicates that there is little irreversible CO₂ adsorption on the wet alumina support, although the appearance of C¹⁶O₂ when C¹⁶O and ¹⁸O₂ are equilibrated over the catalyst suggests that a reversible exchange of CO₂ with adsorbed H₂O or hydroxyl groups is occurring via a reaction such as



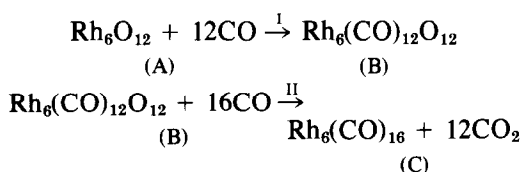
on the wet alumina surface which would exchange O-16 from the water for O-18 in the initial CO₂ product. (This is supported by the final entries in Table 3 which show that the reaction of ^{18,18}O₂ with C¹⁶O over a relatively dry sample with the reactant gases recirculating through a L_{N2} trap resulted in more O-18 remaining in the CO₂ product than a static reaction over a water-saturated sample.) The infrared spectra show that after prolonged exposure to CO the dicarbonyl species is completely converted to Rh₆(CO)₁₆, although not all of the rhodium present has reacted with CO. Identification of Rh₆(CO)₁₆ is based on the similarity of the infrared spectra to that of the parent complex (Table 2), and on the fact that Rh₆(CO)₁₆ can be recovered into refluxing chloroform under an atmosphere of CO (7). We have noticed small variations in the frequency ($\pm 15 \text{ cm}^{-1}$) of the terminal CO band of Rh₆(CO)₁₆. These appear to occur as the extent of hydration of the support changes, and suggest that differences in the extent of hydrogen bonding of the complex to the support are occurring.

The role of water in promoting the carbonylation reaction is interesting. Smith *et al.* (11) have suggested that Rh₆(CO)₁₆ is formed on the surface through a reaction of the type:



in which water is directly involved. (X represents an oxide ion of the support, so that HX is a surface hydroxyl group.) Our experiments showed clearly, however, that ¹⁸O₂, added in the decarbonylation step,

appeared in the CO₂ which was formed. In addition, our volumetric data were not consistent with the above reaction since 3 mol of CO₂ formed for every 4 mol of CO adsorbed when we started from a completely decarbonylated sample. A reaction scheme which does account for the observed stoichiometries is as follows (the molecular nature of the species involved is discussed further below).

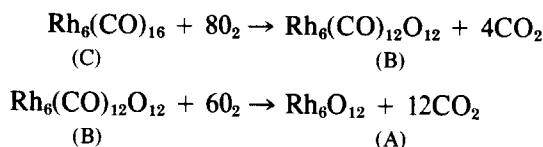


According to this scheme, a ratio of CO adsorbed to CO₂ produced of 1.33 will always be obtained provided all of the intermediate species (B) (which corresponds to the dicarbonyl species suggested by Smith *et al.*) reacts to form (C). Variations in the overall CO₂:Rh and CO:Rh ratios from sample to sample suggest that not all rhodium present could be carbonylated according to the scheme given above. Assuming the above stoichiometry, the

fraction of Rh reacting with CO varied from about 60% at a Rh loading of 0.86% by weight to 40% with the 7.3% Rh sample.

Step I in the proposed scheme is relatively rapid, while step II occurs very slowly unless physically adsorbed H₂O is present on the support. Since direct participation of H₂O in the reaction is ruled out by the absence of H₂ or hydrocarbon product, we may suggest that adsorbed H₂O weakens the interaction between B and the support, thus allowing faster attack of CO on the oxygen ligands to produce CO₂. The possibility of Rh₆(CO)₁₆ being formed within a layer of physically adsorbed H₂O has also been suggested by Smith *et al.* (11).

The reverse reaction, decarbonylation of Rh₆(CO)₁₆ by treatment with O₂, also occurs in two steps. The intermediate dicarbonyl (B) is formed rapidly, accompanied by formation of CO₂. The second step, which occurs more slowly, and which was not observed by Smith *et al.* (11), presumably because their samples were relatively dry, involves disappearance of the dicarbonyl species and further CO₂ formation.



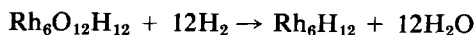
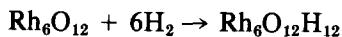
In the absence of physically adsorbed H₂O the second step does not occur to completion and the dicarbonyl species (B) persists. In the presence of H₂O, however, attack of O₂ on the dicarbonyl species is facilitated. One of our isotope experiments (¹⁸O₂ + C¹⁶O ads) suggests that H₂O is not involved directly in the decarbonylation reaction, although this could not be confirmed by measurement of the stoichiometry. Provided a sufficient level of adsorbed water was maintained on the support surface, a sample could be cycled

many times between the fully carbonylated (C) and fully decarbonylated (A) forms.

H₂ Adsorption Experiment

The H₂ adsorption data shown in Fig. 6 provide confirmation of the stoichiometric scheme suggested above. The reaction of H₂ with a fully oxygenated (decarbonylated) sample occurs in two stages, an initial rapid adsorption of H₂ to a maximum extent of about 1 H₂ per Rh, followed by a slow reaction of further H₂ with adsorbed oxygen to produce H₂O. This may be repre-

sented as follows:



Complete reaction of all Rh present would lead to a total H_2 consumption of three molecules per Rh. The experiment shown in Fig. 5 was terminated before H_2 consumption was complete and gave a value of 2.1 H_2 per Rh. About 0.9 H_2 per Rh was involved in the initial rapid adsorption, and the remainder reacts with oxygen to produce H_2O which is adsorbed on the support. The adsorbed H_2 was removed by evacuation at room temperature.

Molecular Nature of the Oxygenated Species

From the infrared spectra alone we cannot determine the nature of the intermediate species (B), other than the fact that it appears to be a dicarbonyl. The identification of the dicarbonyl as $\text{Rh}^{\text{I}}(\text{CO})_2$ by Smith *et al.* (11) is based on the assumption that oxidation necessarily involves destruction of the Rh_6 cluster, although they comment that the oxidized species are probably still weakly bound to each other. The possibility of the dicarbonyl bands arising from a simple oxocluster of the type $\text{Rh}_6\text{O}_x(\text{CO})_{12}$ was suggested for $\text{Rh}_6(\text{CO})_{16}$ on SiO_2 when the sample was treated with O_2 at 100°C (11). Additionally, Gelin *et al.* (14) report that the $\text{Rh}_6(\text{CO})_{16}$ cluster "may be decarbonylated by O_2 or *in vacuo* at 373K without substantial loss of its molecular structure" when the cluster compound is supported on zeolite. In their studies $\text{Rh}_6(\text{CO})_{16}$ was sublimed at 80°C *in vacuo* onto NaY or HY zeolites; the resulting materials were subject to reversible CO/O_2 reactions similar to those described here with stoichiometric quantities of CO_2 formed in the oxygenation step. The oxygenated species was proposed to be a cluster of formula $\text{Rh}_6(\text{O}_2)_8$. The question of whether or not the Rh_6 cluster on Al_2O_3 retains its integrity during the carbonyla-

tion and decarbonylation cycles cannot be finally answered from the evidence available so far. It may be pointed out, however, that the cluster is more likely to remain intact if there is not a strong interaction with the support. Knözinger (17) has shown that $\text{Rh}_6(\text{CO})_{16}$ is degraded to mononuclear Rh species on ligand modified SiO_2 , due to extensive ligand substitution of the $\text{Rh}_6(\text{CO})_{16}$. The reversible carbonylation and decarbonylation cycles described here occur only in the presence of physically adsorbed H_2O . Under such conditions, strong support interactions of the type suggested by Smith *et al.* (11), involving formation of Al-O-Rh bonds, seem unlikely.

It thus appears reasonable to identify the fully and partially decarbonylated species, (A) and (B), as oxoclusters of rhodium. The observation of a molecular exchange between $^{18}\text{O}_2$ and adsorbed oxygen without formation of $^{18}\text{O}^{16}\text{O}$ precludes a reversible dissociative adsorption of oxygen. Furthermore, the reaction of O_2 with adsorbed CO is irreversible, since the $^{18}\text{O}_2$ retained its isotopic label despite the rapid exchange of CO_2 with oxygen on the alumina surface. This suggests that the oxoclusters contain dioxygen ligands. If this suggestion is correct, the Rh- Al_2O_3 system provides an interesting example of nondissociative O_2 adsorption on a small metal atom cluster. Species (B) should then be written $\text{Rh}_6(\text{CO})_{12}(\text{O}_2)_6$, and species (A) as $\text{Rh}_6(\text{O}_2)_6$. The nature of the adsorbed O_2 is under further investigation in this laboratory. Experiments with techniques which observe the Rh coordination sphere directly, such as EXAFS (25, 26), or low-frequency laser Raman spectroscopy (27) are needed to prove the existence (or otherwise) of the oxoclusters.

Thermal Stability

Outgassing adsorbed $\text{Rh}_6(\text{CO})_{16}$ at 150°C results in complete loss of bridging carbonyl ligands, but exposure to CO and H_2O (to replace physically adsorbed H_2O lost during outgassing) restores the $\text{Rh}_6(\text{CO})_{16}$

spectrum. Provided sufficient H_2O is present, the catalyst outgassed at 150°C will undergo the same carbonylation and oxygenation cycles as are observed with samples treated only at room temperature. Outgassing at 250°C (or higher) decarbonylated the sample completely and destroyed the ability of the catalyst to reform $\text{Rh}_6(\text{CO})_{16}$. This treatment evidently resulted in irreversible destruction of the Rh_6 cluster. The carbonyl bands observed (Fig. 10) when CO is adsorbed on a sample treated at 250°C are very similar to those obtained from highly dispersed conventional rhodium catalysts (20–22) and are about 15 cm^{-1} higher in frequency than the dicarbonyl bands we observe for species (B). We have at no time observed the carbonyl bands typical of CO adsorbed on large Rh clusters (a bridging band at 1870 cm^{-1} and terminal band at 2070 cm^{-1} (20)) when CO is adsorbed on $\text{Rh}_6(\text{CO})_{16}\text{-Al}_2\text{O}_3$ which has been heated *in vacuo*. This is consistent with the absence of recognizable metal particles in the electron micrographs. A very high dispersion of Rh is evidently maintained after decomposition of the Rh_6 clusters *in vacuo*. In contrast, decomposition of the clusters by heating in H_2 does result in carbonyl bands more characteristic of larger clusters (11).

CONCLUSIONS

The investigations reported here complement the earlier studies, and lead to some interesting conclusions regarding the chemistry of $\text{Rh}_6(\text{CO})_{16}$ on alumina. The major difference between the model developed here and that presented by Smith *et al.* (11) lies in the strength of the support interaction. We believe that the facile reversibility of the carbonylation–decarbonylation cycles, in which physically adsorbed water plays a key role, rules out the oxidation and resulting destruction of the cluster by hydroxyl groups suggested by Smith *et al.* (11). Nevertheless, some interaction with the support is essential to the chemistry observed since similar behavior is not ob-

served in solution or on SiO_2 . The loss of reversibility on heating *in vacuo* at 250°C or higher may be due to oxidation of the cluster, but this is not accompanied by appreciable sintering.

The reproducible stoichiometry for CO adsorption and CO_2 formation, and the absence of isotopic scrambling between $^{16}\text{O}_2$ and $^{18}\text{O}_2$, suggests that the fully decarbonylated clusters contain dioxygen ligands and may be written $\text{Rh}_6(\text{O}_2)_6$. The nature of the two-step carbonylation process for the oxygenated cluster suggests the dioxygen ligands are in bridging positions on the cluster.

Finally, all work reported on the $\text{Rh}_6(\text{CO})_{16}/\text{Al}_2\text{O}_3$ system points to its unique nature relative to conventional supported Rh catalysts. This is demonstrated by the facile room temperature carbonylation cycle, the reproducible stoichiometry of CO_2 formation, the absence of larger crystallite formation up to 450°C , the maintenance of low or zero oxidation state throughout the several steps observed here, and the high state of “dispersion” even for relatively high loadings. These observations point to the need for further study of catalytic and other properties of this interesting system.

ACKNOWLEDGMENTS

Acknowledgment is made to Dr. Gus Apai and Mr. John Hamilton of Eastman Kodak Research Laboratories for obtaining transmission electron micrographs and for providing helpful discussions, and to the Donors of the Petroleum Research Fund, administered by the American Chemical Society, for partial support of this research. This research was also supported by grant #CHE77-20373 from the National Science Foundation.

REFERENCES

1. Muetterties, E. L., *Science* **196**, 839 (1977) and references therein.
2. Ichikawa, M., *J. Chem. Soc. Chem. Commun.* 26 (1976); 11 (1976); 566 (1978); *Bull. Chem. Soc. Japan* **51**, 2268 (1978).
3. Knözinger, H., and Rumpf, E., *Inorg. Chim. Acta* **30**, 51 (1978).
4. Jarrell, M. S., and Gates, B. C., *J. Catal.* **54**, 81 (1978).

5. Anderson, J. R., and Mainwaring, D. E., *J. Catal.* **35**, 162 (1974); Anderson, J. R., Elmes, P. S., Howe, R. F., and Mainwaring, D. E., *J. Catal.* **50**, 508 (1977).
6. Mantovani, E., Palladino, N., and Zanobi, A., *J. Mol. Catal.* **3**, 285 (1977).
7. Smith, G. C., Chojnacki, T. P., Dasgupta, S. R., Iwatate, K., and Watters, K. L., *Inorg. Chem.* **14**, 1419 (1975).
8. Anderson, J. R., and Howe, R. F., *Nature (London)* **268**, 129 (1977).
9. Howe, R. F., *J. Catal.* **50**, 196 (1977); *Inorg. Chem.* **15**, 486 (1976).
10. Kazusaka, A., and Howe, R. F., *J. Mol. Catal.*, in press (and references therein).
11. Smith, A. K., Hugues, F., Theolier, A., Basset, J. M., Ugo, R., Zandereghi, G. M., Bilhou, J. L., Bilhou-Bougnol, V., and Graydon, W. F., *Inorg. Chem.* **18**, 3105 (1979).
12. Brenner, A., and Burwell, R. L., Jr., *J. Catal.* **52**, 353 (1978); *J. Amer. Chem. Soc.* **97**, 2565 (1975).
13. Brenner, A., *J. Chem. Soc. Chem. Commun.* 251 (1979); *Inorg. Chem.* **18**, 2836 (1979).
14. Gelin, P., BenTaarit, Y., and Naccache, C., *J. Catal.* **59**, 357 (1979).
15. Couderier, G., Gallezot, P., Praliand, H., Primet, M., and Imelik, B., *C. R. Acad. Sci. Paris C* **282**, 311 (1976).
16. Smith, A. K., Theolier, A., Basset, J. M., Ugo, R., Commereuc, D., and Chauwin, Y., *J. Amer. Chem. Soc.* **100**, 2590 (1978).
17. Knözinger, H., Thornton, E. W., and Wolf, M., *J. Chem. Soc., Trans. Faraday Soc.* 1888 (1979).
18. Chini, P., and Martinengo, S., *Inorg. Chim Acta* **3**, 315 (1969).
19. Naccache, C., BenTaarit, Y., and Boudart, M., Proc. 4th Int. Conf. Molecular Sieves, 1977, 144 (ACS Symp. Ser. 40).
20. Bjorklund, R. B., and Burwell, R. L., Jr., *J. Colloid Interface Sci.* **70**, 383 (1979).
21. Yates, J. T., Jr., Duncan, T. M., and Vaughan, R. W., *J. Chem. Phys.* **71**, 3908 (1979).
22. Yates, D. J. C., Murrell, L. L., and Prestridge, E. B., *J. Catal.* **57**, 41 (1979).
23. Primet, M., *J. Chem. Soc. Faraday Trans. I* **74**, 2570 (1978).
24. Primet, M., Vedrine, J. C., and Naccache, C., *J. Mol. Catal.* **4**, 411 (1978).
25. Reed, J., Eisenberger, P., Teo, P. K., and Kincaid, B. M., *J. Amer. Chem. Soc.* **100**, 2375 (1978).
26. Via, G. H., Sinfelt, J. H., and Lytle, F. W., *J. Chem. Phys.* **71**, 690 (1979).
27. Kettle, S. F. A., and Stanghelline, P. L., *J. Amer. Chem. Soc.* **101**, 2749 (1979).
28. Kaesz, H. D., Knox, S. A. R., Koepke, J. W., and Sallant, R. B., *Chem. Commun.* 477 (1971).
29. L'Eplattenier, F., and Calderazzo, F., *Inorg. Chem.* **6**, 2092 (1967).